Pharm Res (2014) 31:3191–3200
DOI 10.1007/s11095-014-1411-6

RESEARCH PAPER

A New Twist in the Old Story-can Compression Induce Mixing of Phase Separated Solid Dispersions? A Case Study of Spray-Dried Miconazole-PVP VA64 Solid Dispersions

Abhishek Singh • Jan Van Humbeeck • Guy Van den Mooter

Received: 2 January 2014 / Accepted: 6 May 2014 / Published online: 22 May 2014

ABSTRACT

Purpose The phase response of Miconazole-PVP VA64 solid dispersions upon compression was investigated. This would allow understanding the phase behavior of these solid dispersions upon application of a different kind of stress (other than humidity and temperature) and ultimately lead to mechanistic perception of the phase changes taking place.

Methods Miconazole and PVP VA64 were chosen as a model drug and polymer, respectively and solid dispersions were prepared by spray drying. Dried solid dispersions were compressed using different compression pressure but constant dwell time. MDSC and XRPD were used to characterize and study the effect of compression on the system.

Results The solid dispersions showed a single T_g till 20% drug loading after which two T_g's were observed. Application of compression to the phase separated 30 and 40% compositions induced mixing resulting in only a single T_g. This reduction in number of T_g's upon compression is a result of mixing which can be attributed to polymer flow resulting in reduction of the domain size of different phases in the solid dispersions.

Conclusions Application of compression can influence the phase behavior of Miconazole-PVP VA64 solid dispersions. This observation may have drastic impact on the formulation development approach for solid dispersions to be administered as tablets.

KEY WORDS amorphous solid dispersions · compression · miconazole · phase separation · polymer flow

A. Singh • G. Van den Mooter (✉)
Drug Delivery and Disposition, Department of Pharmaceutical and Pharmacological Sciences, University of Leuven, Campus Gasthuisberg O+N2 Herestraat 49 b921, 3000 Leuven, Belgium
e-mail: guy.vandenmooter@pharm.kuleuven.be

J. Van Humbeeck
Surface and Interface Engineered Materials, Department of Metallurgy and Materials Engineering, University of Leuven, Campus Arenberg Kasteelpark Arenberg 44 b2450, Leuven 3001, Belgium

ABBREVIATIONS

API	Active pharmaceutical ingredient
ASD	Amorphous solid dispersions
ΔCp	Heat capacity
ΔH_f	Heat of fusion
MDSC	Modulated differential scanning calorimetry
PVP K25	Polyvinylpyrrolidone K25
PVP VA64	Poly (1-vinylpyrrolidone-co-vinyl acetate)
RCS 90	Refrigerated cooling system
T_g	Glass transition temperature
ΔT_g	Width of the glass transition temperature
T_m	Melting point
ΔT_m	Melting point depression

INTRODUCTION

Poor aqueous solubility of the active pharmaceutical ingredient (API) has been reverberated since many years in numerous articles as one of the biggest challenges currently faced by formulation scientists. The trend doesn't seem to abate with advances in drug design techniques driving the molecular structures towards further complexity (1). The poor solubility of the API may arise either due to strong-intermolecular bonding between the molecules ('Brick-dust' compounds) or problems with solvation ('Grease-ball' compounds). Amongst a few approaches available to improve the solubility of these 'Brick-dust' compounds is amorphous solid dispersions (ASD) formulation. As evident by the name these solid dispersions are amorphous and hence no energy is required to break the crystal lattice structure thus increasing solubility. The carrier chosen plays a crucial role by enhancing the wettability and preventing nucleation/precipitation of the drug thereby maintaining the solubility advantage (2).

The choice of a suitable drug delivery platform for any formulation strategy is determined by patient and formulation related factors. Patient related factors such as ease of administration, compliance and cost undoubtedly indicate oral administration of ASD as the preferred route. Not surprisingly most of the marketed formulations (if not all) of solid dispersions till now have been either tablets or capsules which illustrates their popularity from the perspective of both patient and industry (2). However, formulation related factors for ASD are intricate. ASD are particularly vulnerable to moisture consequently ruling out water based liquid formulations. Even the capsule shells containing 4–16% moisture maybe detrimental for ASD stability especially when very hygroscopic polymers are used (3, 4). Also, the bulk density of spray dried ASD is high thereby making capsule filling a difficult operation especially when dose size is high.

Tablets can be used to circumvent the above mentioned dosage form design challenges posed by capsules. Yet tablets do pose a different gamut of problems. It is well known that various unit operations required to prepare an ASD dosage form can be detrimental for its stability. Unit operations involving stress conditions such as high temperature and moisture can potentially result in amorphous-amorphous phase separation or crystallization. However, there is scarce evidence and understanding as to how a different kind of stress such as compression can influence the two main stabilization mechanisms of ASD i.e. intermolecular interactions and anti-plasticization effect of the polymer.

Our research group has been investigating the compression step in tabletting and found out that compression resulted in altered physical stability of melt-cooled amorphous indomethacin. Compression resulted in a significantly high heat of crystallization and lower crystallization temperature indicating not only induction but also an increased extent of crystallization (5). In another study, compression resulted in phase separation of spray-dried metastable Naproxen-Polyvinylpyrrolidone K25 (PVP K25) solid dispersions. This result was ascribed to compression induced conformational changes in hydrogen bonded PVP thereby snapping the weak interaction between the carbonyl of PVP and the hydroxyl of the carboxylic moiety of naproxen (6).

However, it is also pertinent here to ponder upon the consequences of compression on ASD which are devoid of stabilization via H-bonding. This is an unchartered territory and in this stead we decided to investigate the effect of compression on ASD of Miconazole and Poly (1-vinylpyrrolidone-co-vinyl acetate) (PVP VA64) which are both H-acceptors and cannot form hydrogen bonds with each other. The results of this study would hence aid in reflecting upon not only the compression induced phase behavior alteration but also retrospectively on the significance of H-bonding in determining the phase behavior of ASD upon compression. The main focus of this study was on perturbation of the thermal markers (glass transition temperature- T_g, number of T_g's, melting point- T_m and heat of fusion-ΔH_f) of Miconazole-PVPVA64 solid dispersions, Miconazole-PVPVA64 physical mixtures, pure Miconazole and pure PVP VA64. The knowledge about altered thermal markers will help in getting a bulk level idea about the phase behavior which will assist in the eventual mechanistic explanation for the observations.

MATERIALS AND METHODS

Materials

Miconazole was kindly donated by Janssen Pharmaceutica (Beerse, Belgium). Poly (1-vinylpyrrolidone-co-vinyl acetate) (PVP VA64) was purchased from BASF (Ludwisshafen, Germany). All other chemicals and solvents used were of analytical or HPLC grade and were used as received.

Methods

Preparation of Solid Dispersions

A Buchi mini spray-dryer B191 (Buchi, Flawil, Switzerland) was used to prepare solid dispersions with 10%, 20%, 30% and 40% (w/w) of miconazole in PVP VA64. Same process parameters of 60°C inlet temperature, 0.56 m^3/min drying air flow rate, 25 L/min nozzle air flow rate, 6.8 ml/min feed rate, 0.5 mm diameter nozzle tip, 5% feed concentration in dichloromethane were used for all compositions.

Preparation of Physical Mixtures

50%, 60%, 70%, 80% and 90% physical mixtures were prepared by accurately weighing and geometrically mixing Miconazole and PVP VA64.

Thermal Analysis

A Q2000 Modulated differential scanning calorimeter (MDSC) (TA Instruments, Leatherhead, UK) purged with inert dry nitrogen gas at a flow rate of 50 mL/min and connected to a refrigerated cooling system (RCS90) was used to analyze the uncompressed and compressed samples. The calibration was performed for two temperature points using standard indium and octadecane. Melting enthalpy was calibrated and also validated using indium. Heat capacity was calibrated and validated using a sapphire disk by comparing the heat capacity at 66.85°C with modulation amplitude of 0.636°C every 40 s. The samples were crimped in a TA Instruments aluminum pan and subjected to an underlying heating rate of 2°C/min. All samples were analyzed in triplicate. The acquired data was analyzed using Universal Analysis

software (version 4.4, TA Instruments, Leatherhead, UK). Wherever required Origin 8.6 (OriginLab Corp., Northampton, U.S.A.) was also used to plot thermograms.

In order to ensure representative samples for the MDSC analysis of uncompressed physical mixture, PVP VA64 and miconazole were geometrically mixed to make up 10 mg quantity and completely transferred into a PerkinElmer aluminium pan.

Powder X-ray Diffraction (PXRD)

An automated X'pert PRO diffractometer (PANalytical, Almelo, the Netherlands) was used to analyze samples. A copper tube and generator set at 45 KV and 40 mA was employed. All samples were analyzed between 2θ of 4–40° in reflection mode on a zero background plate using 0.0167° step size and 200 s counting time. The continuous data acquisition was done using X'pert Data Collector (PANalytical, Almelo, the Netherlands) and the X'Pert Data Viewer and X'Pert HighScore Plus (PANalytical, Almelo, the Netherlands) were used for data analysis.

Compression

Compression was performed using a manual tablet press RQPBA15 (Rodac International, Sittard, the Netherlands) with a die cavity of 13 mm diameter. 100 mg of sample was placed in the die cavity and compressed using pressures of 188, 564 and 1,129 MPa for a uniform dwell time of 60 s.

Drug Content

Drug content in the solid dispersions was analyzed using HPLC. Approximately 10 mg of the solid dispersion was dissolved in 10 ml DMSO and a series of dilutions was prepared. HPLC analysis was performed in triplicate with a Merck Hitachi pump (L7100), ultraviolet (UV) detector (L7400), autosampler (L7200), interface (D7000) and a LiChrospher 60 RP Select-B C-18 (5 μm, 12.5×4) column (all Merck, Darmstadt, Germany). Isocratic elution mode was employed with a mobile phase made up of Acetonitrile and sodium acetate buffer (pH=3.5 and 25 mM) in 60:40 ratio (v/v) at a flow rate of 1 ml/min. Detection wavelength and injection volume were set at 237 nm and 10 μl, respectively.

Statistical Analysis

The sets of data obtained from this study were tested for significant differences using a student *t*-test. The two different sets of data were considered as independent (unpaired) groups with different variance and without prior knowledge of the direction of the prediction. The student *t*-test was performed using Microsoft Excel 2007 (Microsoft Corp., USA). Difference was considered significant if $p<0.05$.

RESULTS

Compression of Pure Miconazole

Pure miconazole was analyzed using MDSC and the T_m and ΔH_f were determined from the endothermic peak integration of the total heat flow signal. The thermogram had a characteristic sharp endothermic peak and was devoid of any glass transition event. As shown in Fig. 1 the T_m and ΔH_f of uncompressed miconazole were found to be 83.7°C and 90.1 J/g respectively. Upon compression the T_m decreases slightly (between 1.0 and 1.6°C) but is only statistically significant ($p<0.05$) as compared to the uncompressed miconazole for the intermediate and high compression pressure. Another consequence of compression was a statistically significant reduction in the ΔH_f values for all compression pressures i.e. 188, 564 and 1,129 MPa in the range of 7.8–10.0 J/g. Increasing the compression pressure had no statistically significant impact on the T_m and ΔH_f of the compressed samples. XRD analyses of the samples reveal a typical diffractogram (Fig. 2) for a crystalline material with Bragg peaks. Compression results in peak fusion of some of the neighboring Bragg peaks at 2θ values of (14.6°; 14.9°), (19.1°; 19.4°), (24.4°; 24.8°; 25.2°; 25.5°; 26.2°), (27.8°;28.1°) and almost

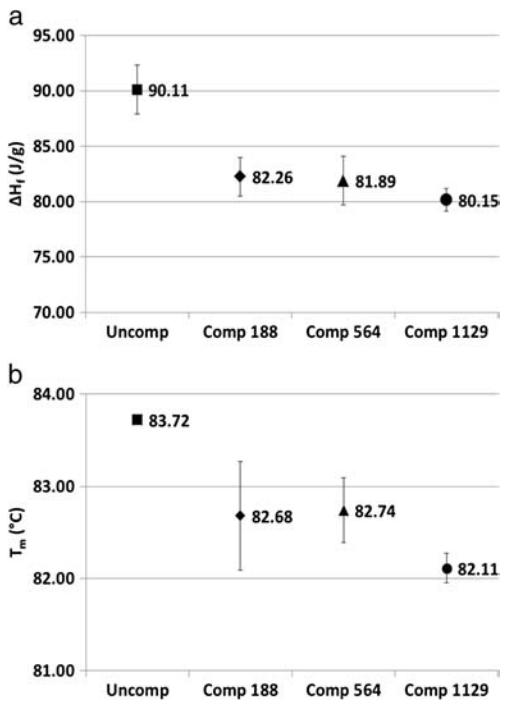

Fig. 1 Plot of ΔH_f (J/g) **(a)** and T_m Onset (°C) **(b)** obtained by DSC analysis of uncompressed miconazole (■) and miconazole compressed at various compression pressure i.e. 188 MPa (♦), 564 MPa (▲) and 1,129 MPa (●). ($n=3$).

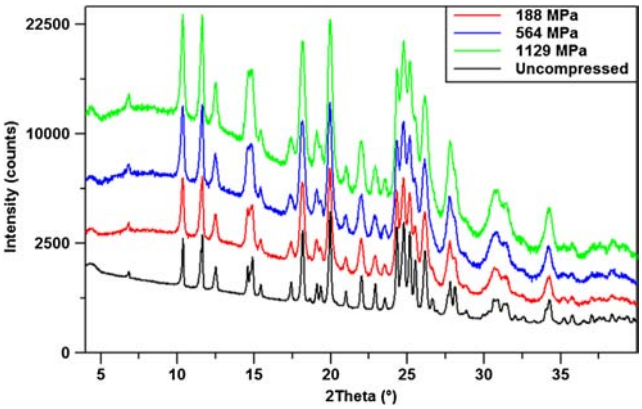

Fig. 2 XRD diffractograms of uncompressed miconazole and miconazole compressed at various compression pressures i.e. 188 MPa, 564 MPa and 1,129 MPa.

total disappearance of the peaks at 26.7°, 28.9°, 32.1° and 32.6°. No peak shifts are observed. Interestingly the peak intensities decrease in a compression pressure dependent manner along with occurrence of an amorphous halo.

Compression of PVPVA64

Assessment of the reversing heat flow signal obtained from MDSC analysis of PVP VA64 revealed a step change in specific heat capacity at 106.8°C recognized as glass transition temperature. The width of the glass transition (ΔT_g) of PVP VA64 was fairly narrow having a value of 14.1°C. Upon compression the T_g of PVP VA64 increased by 1.0 to 1.6°C (Fig. 3a) and ΔT_g varied in the range between 0.4 and 1.3°C (Fig. 3b). No clear trend and statistical differences could be identified, however, due to high standard deviations associated with each data series especially with the compressed samples. The standard deviations for the uncompressed PVP VA64 samples was 0.2°C as opposed to 1.1, 1.5 and 1.3°C for samples compressed at 188, 564 and 1,129 MPa respectively. XRD diffractograms of the uncompressed and compressed PVP VA64 showed no changes in the diffraction pattern (Fig. 4).

Compression of Physical Mixtures

The uncompressed physical mixtures of miconazole-PVP VA64 did not exhibit any drug composition dependent depression in melting point (ΔT_m) as shown in Fig. 5. Compression results in an increase in melting point depression in the range of 0.8 to 2.3 K, 1.1 to 2.4 K and 1.5 to 2.6 K for 188, 564 and 1,129 MPa respectively. Smallest increase in the ΔT_m is for the 90% drug loaded physical mixtures. Moreover, increasing compression pressure did not increase the ΔT_m significantly.

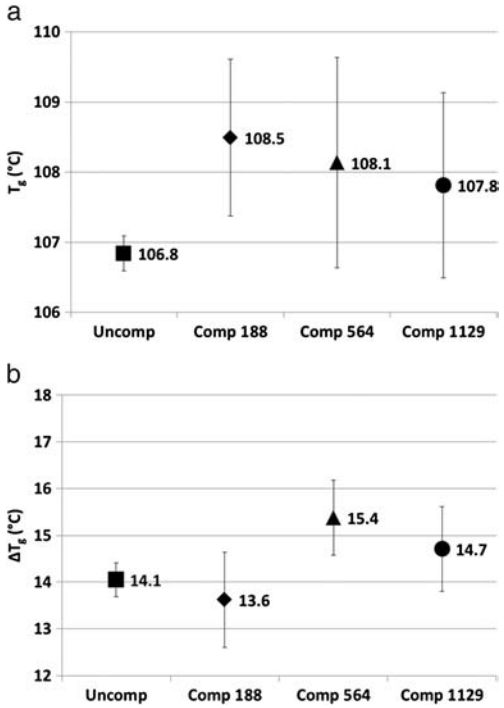

Fig. 3 Plot of T_g (°C) **(a)** and ΔT_g (°C) **(b)** obtained by DSC analysis for uncompressed PVP VA64 (■) and PVP VA64 compressed at various compression pressure i.e. 188 MPa (♦), 564 MPa (▲) and 1,129 MPa (●). ($n = 6$).

Compression of Solid Dispersions

As depicted in the Fig. 6 the T_g of the system decreases from 91.8 to 72.8°C and the ΔT_g increases from 25.4 to 37.3°C as the drug content in the solid dispersion increases from 10% to 20%. The DSC thermograms of 10 and 20% compositions showed a single T_g accompanied by a composition dependent increase in the ΔT_g of the system indicating increasing heterogeneity. Phase separation into the drug rich and the polymer rich phase is clearly interpretable from the presence of two distinct T_g's for the 30 and 40% compositions as depicted in Fig. 7. The higher T_g of 80.5°C and 70.0°C for the 30 and

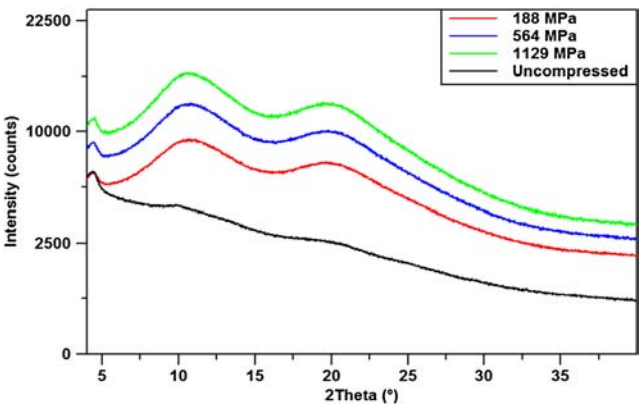

Fig. 4 XRD diffractograms of uncompressed PVP VA64 and PVP VA64 compressed at various compression pressures i.e. 188 MPa, 564 MPa and 1129 MPa.

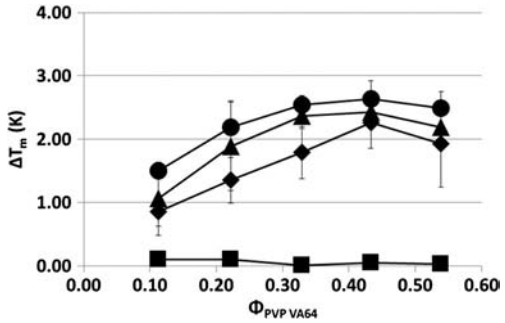

Fig. 5 Plot of ΔT_m (K) vs $\Phi_{PVP\ VA64}$ obtained by DSC analysis of various compositions of uncompressed physical mixtures (■) as well as physical mixtures compressed at various compression pressure i.e. 188 MPa (♦), 564 MPa (▲) and 1129 MPa (●). ($n = 3$).

40% compositions respectively corresponds to the polymer rich phase. The lower T_g of 44.7°C and 32.0°C for the 30 and 40% compositions respectively, corresponds to the drug rich phase. Upon compression of the 10 and 20% drug loaded solid dispersion no difference is observed between the uncompressed samples and the compressed samples. Increasing the compression pressure from 188 to 1,129 MPa also does not lead to any statistically significant changes in the thermal markers. Strikingly, upon compression of the 30 and 40% composition the second phase T_g disappears and only one T_g is observed as shown in Fig. 7. The compression of the 30% composition was done using only two pressures 564 and 1,129 MPa. The new single T_g values of the 30% composition

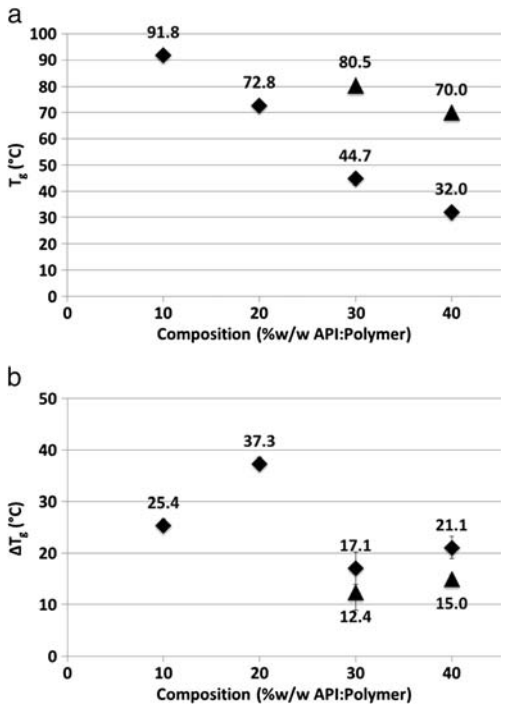

Fig. 6 Plot of T_g vs composition (%w/w API:Polymer) **(a)** and ΔT_g (°C) vs composition (%w/w API:Polymer) **(b)** obtained by DSC analysis of solid dispersions representing T_g and ΔT_g values for drug rich phase (♦) and polymer rich phase (▲).

obtained upon compression by 564 MPa and 1,129 MPa are 52.9 and 52.8°C respectively. These values lie between the two T_g's (44.7 and 80.4°C) of the uncompressed 30% composition. The new single T_g values of the 40% composition obtained upon compression by 188, 564 and 1,129 MPa are 38.2, 39.4 and 37.7°C respectively. These values also lie between the initial two T_g's (32.0 and 70.0°C) of the uncompressed 40% composition. Comparing the combined ΔT_g values (29.5°C) of the drug rich and polymer rich phase present in the uncompressed 30% composition to the ΔT_g value of the single phase system obtained upon compression using 564 MPa (27.1°C) and 1,129 MPa (27.7°C) indicates no significant difference. But for the 40% composition, comparison between the combined ΔT_g values (36.1°C) of the drug rich and polymer rich phase present in the uncompressed sample to the ΔT_g value of the single phase system obtained upon compression using 188 MPa (31.0)°C, 564 MPa (28.9°C) and 1,129 MPa (28.9°C) reveals a reduction upon compression.

The XRD diffractograms of the uncompressed and the compressed solid dispersions (Fig. 8a and b) are devoid of any Bragg peaks and characterized by an amorphous halo pattern thereby indicating that all the samples are X-ray amorphous before as well as after compression. These XRD results are in congruence with the MDSC findings. For all the compositions comparison of the diffractograms of the uncompressed and compressed solid dispersions (Fig. 8c and d) reveal an aberration in the halo peak at the 2Theta value of 12–13°.

DISCUSSION

Various unit operations during tablet development can result in process-induced solid state alterations of the tablet constituents thereby jeopardizing the performance of the final product. This aspect has been explored widely for the crystalline materials and there are several reports about the compression induced phase transformation (7). The story is not the same for amorphous systems which are marred by instability warranting a specialized dosage form such as a solid dispersion. Significant attention has been paid to the effect of storage conditions (temperature and relative humidity) on solid dispersions (8). But the effect of a different kind of stressor i.e. compression on solid dispersions is largely ignored. It is not difficult to comprehend the fact that even a slight alteration in the phase behavior (presence as a single mixed phase to an amorphous-amorphous/amorphous-crystalline phase separated system) maybe enough to put at risk the critical quality attributes of the final formulation viz. stability, dissolution rate and eventually bioavailability. Therefore it is imperative to investigate the effect of various steps involved in tableting on solid dispersions.

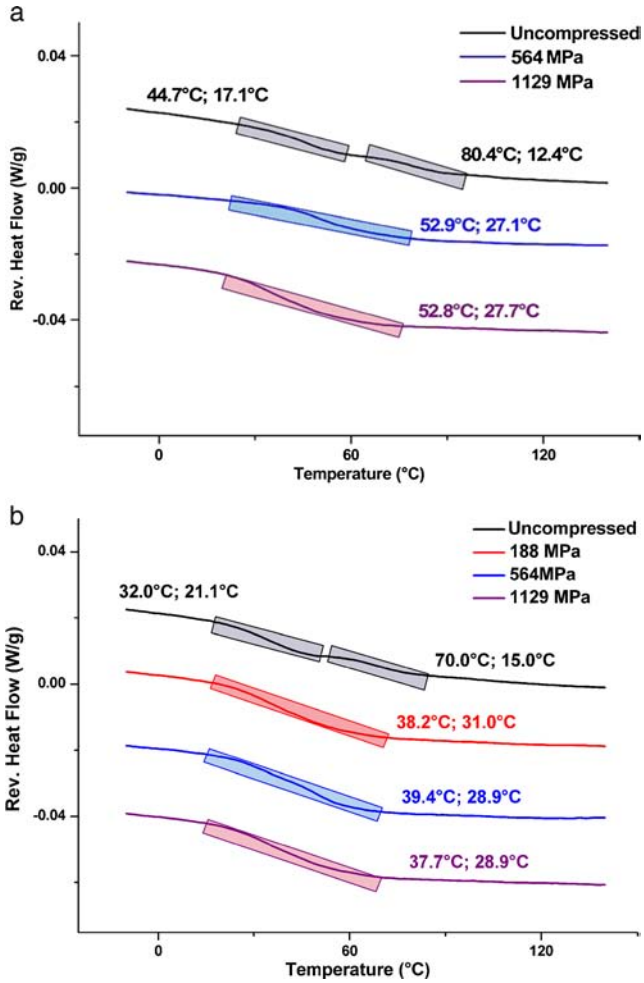

Fig. 7 DSC thermogram plots of Rev. Heat flow (W/g) vs Temperature (°C) showing the presence of two distinct T_g's for the 30% **(a)** and 40% **(b)** composition (%w/w API:Polymer) and subsequent mixing of the system resulting in a single T_g upon application of compression pressure. First value in the data labels next to the glass transitions enclosed in the boxes is T_g and the second value is the ΔT_g.

During tableting the compaction step is one of the most important steps involving transfer of mechanical energy to the powder mass eventually resulting in the formation of a compact. The work done on the powder mass results in the particle rearrangement followed by deformation of materials and ultimately the formation of a compact mediated by electrostatic forces, van der Waals forces and H-bonding (9). H-bonding between the API and polymer also plays a crucial role in stabilization of solid dispersions apart from the antiplasticization effect (10, 11). It has been already reported that compression can result in the phase separation of naproxen-PVP solid dispersions. This system is capable of forming H-bonds between the carbonyl of PVP and the hydroxyl of the carboxylic moiety of naproxen. Upon compression the hydrogen bonds are compromised resulting in the demixing of the system (6). But the solid dispersions which are stabilized only by the antiplasticization effect of the polymers will certainly be devoid of any hydrogen bonding alteration mediated phase behavior changes and any changes may be associated with the miscibility between the API and the polymer. For this study miconazole and PVP VA64 were chosen as the components of the binary solid dispersions because they both are H-acceptors thereby ruling out the opportunity of hydrogen bonding with each other upon spray drying and further compression.

The T_g of the amorphous miconazole generated by quench cooling and PVP VA64 is 2.1°C and 106.7°C respectively. All the DSC thermograms of the solid dispersions were devoid of any endothermic melting peaks indicating that the spray dried product was amorphous. This was also confirmed by the presence of only broad scattering peaks corresponding to the amorphous substance and absence of any sharp Bragg peaks in the XRPD diffractograms of the solid dispersions.

In accordance with the Gordon Taylor equation which predicts the T_g of ideally mixed binary systems, the final T_g of the solid dispersions lied between that of the pure components (12). Solid dispersions having miconazole loading up to 20% showed only one single T_g which decreased as the amount of amorphous miconazole in the solid dispersions was increased upon increasing the drug loading. The width of the T_g of the amorphous system is an indicator of the heterogeneity and therefore miscibility of the system (13). An increase in the ΔT_g was observed up to 20% miconazole loading because of an increased heterogeneity in the solid dispersions. This is also exemplified by the fact that a further increase in the miconazole loading to 30 and 40% resulted in phase separation and registering of two T_g's which could be clearly seen in the reversing heat flow signal of the MDSC thermograms. The higher T_g values correspond to that of a polymer rich phase because of high T_g of PVP VA64 and the lower T_g values correspond to the drug rich phase due to low T_g of miconazole. The 40% compositions had lower values for both the drug-rich and the polymer-rich phase T_g as compared to the 30% composition due to increased amorphous miconazole content.

The glass transition marks an abrupt discontinuity in the enthalpy, entropy and the volume of the material relative to the quasi-equilibrium line to attain non-equilibrium glassy consistency. MDSC detects this as a step change in heat capacity and it is possible to calculate the T_g and change in heat capacity associated with the transition from the reversing heat flow signal recorded by MDSC. Glass transition occurs due to freezing of global molecular motions and hence a single T_g indicates that the similar domains in the bulk sample undergo a global change in the molecular motions in the same temperature range within a similar time-frame indicating similar composition. Occurrence of two separate T_g's indicate two separate domains for which the change in global molecular motions occur at different temperatures. These separate domains have different API: polymer ratio translating in

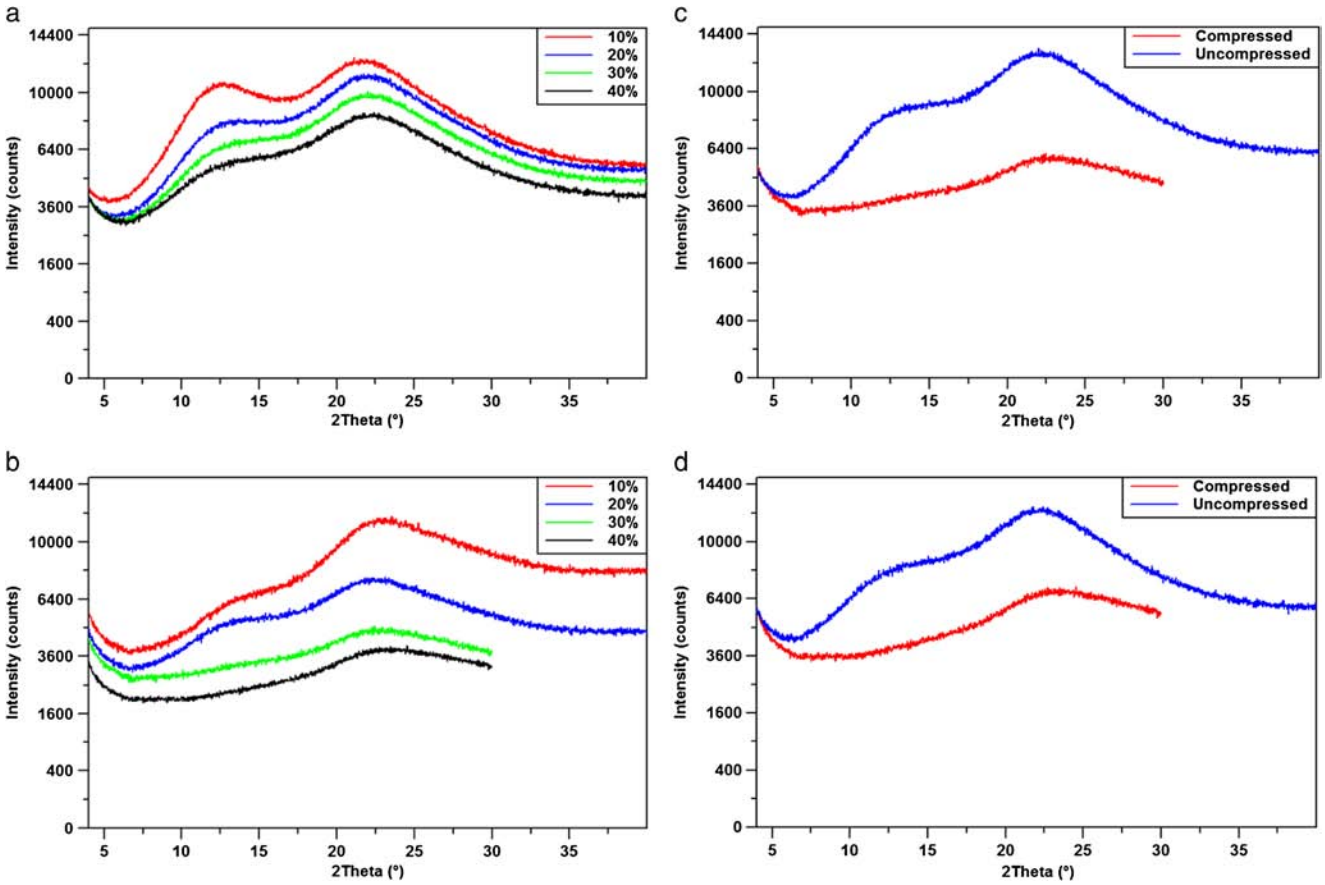

Fig. 8 XRD diffractograms of uncompressed **(a)** and compressed (188 MPa) **(b)** solid dispersions of various compositions. Comparison between the uncompressed and the compressed samples for the 30% **(c)** and 40% **(d)** compositions is shown.

different miscibility and hence inadequate crystallization inhibition of the API is very much possible in the API rich domain where the API molecules are abundant and can possibly form nuclei. The amorphous-amorphous phase separated system will maintain its solubility advantage over the crystalline counterpart of the API but maybe more prone to instability. Hence when applying compression pressure to the solid dispersions it is important to observe the impact of the pressure on the number of T_g's of the solid dispersions.

The compositions which showed only one T_g were not affected by compression. Or in other words the systems where the drug was already well mixed in the polymer matrix did not undergo further mixing or demixing which could be detected by MDSC. Interestingly, the solid dispersions having two T_g's initially showed only one T_g upon compression. To the best knowledge of the authors mixing of solid dispersions upon compression has never been reported in the literature before. Any change in the miscibility of the solid dispersions would involve change in the microstructure which is reflected in the XRPD diffractogram as reduction in the intensity of peak at 2θ value of 12–13° of the compressed samples as compared to the uncompressed solid dispersions (Fig. 8). Although no detailed information about the amorphous domains can be derived from this data, it leads to inference that compression results in microstructure alteration. However it should be kept in mind that microstructure change indicated by the peak intensity variations will not necessarily be reflected as mixing effect indicative by change in number of T_g's. This is clear by the observation that 10 and 20% solid dispersions which show no change in T_g or ΔT_g upon compression do show changes in PXRD pattern (Table I).

The microstructure of solid dispersions consists of miconazole molecules dispersed in the PVP VA64 polymer matrix. The uncompressed solid dispersions can be represented as shown in the Fig. 9a where a magnified view is shown. The domains in the powder mass are those which are rich in miconazole and the others which are rich in PVP VA64. These phase separated regions should have a size of ca. >30 nm to be measured and detected as separate events in MDSC (14). For the 30% and 40% uncompressed Miconazole-PVPVA64 solid dispersions the presence of two T_g's indicates the presence of miconazole rich and PVP VA64 rich domains which are >30 nm in size to be detected by the MDSC. Interestingly upon compression Miconazole-PVP VA64 solid dispersions show only one T_g as represented in Fig. 9b. Observation of only a single T_g points to the fact that

Table I The Table Enlists Thermal Markers of the Solid Dispersions i.e. Number of T_g's Both Before and After Compression. Also Mentioned is the Effect of Compression on the ΔT_g Value

Composition % (w/w)	Uncompressed	Effect of compression on	
		T_g	ΔT_g
10	Single T_g 91.8°C	—	—
20	Single T_g 72.8°C	—	—
30	Two T_g 44.7°C, 80.5°C	Single T_g 564MPa: 52.9°C 1129MPa: 52.8°C	NA*
40	Two T_g 32.0°C, 70.0°C	Single T_g 188MPa: 38.2°C 564MPa: 39.4°C 1129MPa: 37.7°C	NA*

*NA- Effect of ΔT_g values not mentioned since number of T_g's is different

the size of miconazole rich and PVP VA64 rich domains gets reduced upon compression resulting in only one T_g being observed. Why this reduction in domain size occurs can be explained through deformation under stress of glassy polymers and glassy solid dispersions as such.

When the solid dispersion is subjected to compression pressures of 188 MPa, 564 MPa and 1,129 MPa there is a reduction in bulk volume, particle rearrangement, particle deformation and consolidation ultimately resulting in the formation of compacts. Consolidation may be a major reason behind the increased mechanical strength of the powder bed when it is subjected to rising compression pressure (15). It might have resulted in different tablet parameters for different compression pressures used (188 MPa, 564 MPa and 1,129 MPa) in our study. However, thermal markers such as T_g and ΔT_g of the solid dispersions remained unchanged upon increasing compression pressure thereby indicating that consolidation at increasing compression pressure did not affect the thermal properties of the compact any further and the deformation step may well be responsible for the changes observed. Bulk polymers generally exhibit plastic yielding and PVP VA64 which is an amorphous polymer is not an exception either (16). The deformation mechanism of such polymeric glasses is an active and challenging area of research. Existing knowledge points towards applied stress induced increase in segmental mobility with a resulting decrease in viscosity which eventually allows the polymer glasses to 'flow' (17, 18). How this flow occurs at molecular level is yet to be understood. But it is clear that upon application of sufficient force glassy polymers can undergo up to 1000 fold increase in segmental mobility (19). Several theories have been put forward to explain the deformation mechanisms of the glassy polymers. Early theories postulated the alteration in the energy barriers for structural rearrangements in the solids caused by shear stress which ultimately led to structural changes. It was also proposed that creation of local pockets of material with liquid like molecular mobility takes place due to the flexing of dihedral angles by shear stress. Another model describes the accumulation of rotations of kink pairs along the polymer chain as being responsible for shear strain. Theories based on free volume suggested incorporation of additional volume in the matrix as being responsible for increase in molecular mobility and hence polymer deformation (20). It will be presumptuous to pin-point a single theory to explain our results since the molecular level arrangement of the solid dispersions before and after compression is not clear, let alone what changes occur to the molecular arrangement during compression. Nonetheless it can be postulated that reduction in the free volume upon compression and mobility of the polymer backbone through rotation of the dihedral angles and segmental motion is at least partially responsible for the mixing. Therefore compression results in mobility of the PVP VA64 chains bringing them closer which in turn causes the motion of the embedded miconazole. This ultimately brings the drug and polymer rich regions closer and in due course leads to reduction of the domain size.

Analysis of the melting point depression (ΔT_m) in the physical mixtures of the API and polymer can be used to estimate the drug-polymer miscibility (21). Melting of the pure drug takes place when the chemical potential of the crystalline drug becomes equal to that of molten drug. A miscible drug-polymer system would lead to reduction in the chemical potential of the drug resulting in melting at lower temperatures. The offset temperature of the melting endotherm was used to calculate ΔT_m in order to ensure complete mixing of miconazole and PVP VA64. The goal was to investigate if compression could induce miscibility in the physical mixtures which is reflected by ΔT_m. No ΔT_m was observed for uncompressed physical mixtures meaning that there was no miscibility between miconazole and PVP VA64. An increase in the ΔT_m was observed which was indicative of increased miscibility of the miconazole and PVP VA64 due to compression. ΔT_m was higher when the polymer volume fraction ($\Phi_{PVPVA64}$) was higher in the physical mixtures. This again illustrates the role played by compression induced effects on polymer in mixing.

In order to attribute the increased ΔT_m to mixing between miconazole and PVP VA64 it was important to investigate how the compression would affect the individual components of the physical mixtures i.e. crystalline miconazole and amorphous PVP VA64. Compression of PVP VA64 showed no statistically significant variation in the T_g or ΔT_g values. The MDSC analysis of the compressed PVP VA64 samples was repeated six times and the standard deviation obtained for T_g or ΔT_g was very high in contrast to the non-compressed polymer as depicted in Fig. 3. This high standard deviation is indicative of an inherent inhomogeneity in the properties of

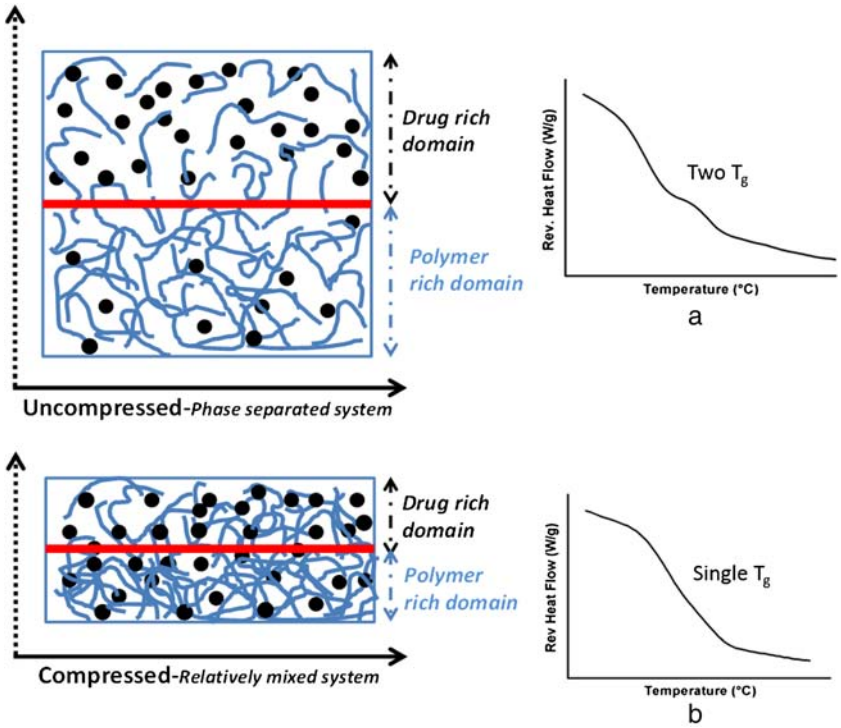

Fig. 9 Illustration depicting the detailed view of uncompressed solid dispersions **(a)** and changes in the amorphous domain structure upon compression **(b)**.

the tablet. This is specifically relevant in our case since a small piece of tablet is isolated from different locations along the periphery of tablet for MDSC analysis. It is a well-known fact that density distribution inside the tablet is not uniform (22). This inhomogeneous density distribution is a reflection of uneven pressure distribution due to interparticle and die wall frictions and reflects in uneven material properties. Compression of crystalline miconazole showed a statistically significant reduction in T_m of around 1.0-1.6°C and reduction in heat of fusion (ΔH_f) of around 7.8–10.0 J/g. The supramolecular arrangement of small organic molecules such as miconazole in condensed phase can be attributed to weak intermolecular forces, hydrogen bonding etc. Upon application of compression, work is done on miconazole crystals thereby raising the overall internal energy. This stress induced increase in the internal energy aids in the disruption of the intermolecular forces and leads to defects in crystal structure. The accumulated crystal defects make it is easy to set in melting (less energy obligation to disrupt the crystal structure) and hence melting point and ΔH_f of miconazole is reduced upon compression. However, a closer look at the XRD data indicates that the reduction of the ΔH_f can have an additional reason other than reduced energy obligation as mentioned above. The XRD diffractograms of miconazole (Fig. 2) reveals a reduction in Bragg peak intensity along with occurrence of an amorphous halo upon compression thereby indicating amorphization of the material. Therefore it can be stated that reduction in ΔH_f of the physical mixtures is due to accumulated crystal defects leading to easy melting and also compression induced amorphization of pure miconazole.

Putting in perspective the results of compression of crystalline miconazole, PVP VA64 and their physical mixtures it can be said that the increased reduction in the T_m of physical mixtures upon compression can be attributed to two factors. First is the effect of compression on pure miconazole which can account for some reduction in the melting point of the physical mixture. However, the magnitude of melting point depression observed for pure miconazole is less than that observed for physical mixtures especially for larger polymer volume fraction and high compression pressure. Therefore it seems that a secondary factor, i.e. miscibility of miconazole in PVP VA64 also accounts for a part of reduction in the T_m of physical mixtures. This is a subsidiary proof that compression can induce mixing in binary systems.

Taking into account all the results it can be said that compression can induce mixing of miconazole-PVP VA64 solid dispersions which can potentially be attributed to polymer flow. This observation can have bearing on solid dispersion formulation development as tablets. It also opens up the avenues of investigating further as to what actually happens to the amorphous domains upon compression and what role additives can play in this scenario.

CONCLUSIONS

In the present study the effect of compression on thermal markers of miconazole-PVP VA64 solid dispersions prepared by spray drying was investigated. Compression had no effect on compositions having lower drug loading and exhibiting

only a single T_g. For the compositions having higher drug loading and showing phase separation, compression resulted in the mixing of the phase separated systems. The absence of a second T_g in the compressed samples can be expounded in terms of reduction of the domain size to <30 nm which cannot be detected any more by MDSC. This reduction in the domain sizes can be potentially attributed to stress induced polymer 'flow' accompanied with free volume reduction which culminates in the better mixing of the spray dried system. This observation may have important consequences as the stabilization of solid dispersions is intricately dependent on the mixing of the API and polymer. Better mixing will enhance crystallization inhibition in the long run.

ACKNOWLEDGMENTS AND DISCLOSURES

The authors acknowledge financial support from FWO-Vlaanderen (G.0764.13). Abhishek Singh acknowledges the financial support via an OT grant number (OT/12/077) from KU Leuven.

REFERENCES

1. Williams HD, Trevaskis NL, Charman SA, Shanker RM, Charman WN, Pouton CW, *et al.* Strategies to address low drug solubility in discovery and development. Pharmacol Rev. 2013;65(1):315–499.
2. Singh A, Worku ZA, Mooter GV. Oral formulation strategies to improve solubility of poorly water-soluble drugs. Expert Opin Drug Deliv. 2011;8(10):1361–78.
3. Podczeck F, Jones BE. Pharmaceutical capsules 2ed. London: Pharmaceutical press; 2004.
4. Chang R-K, Raghavan KS, Hussain MA. A study on gelatin capsule brittleness: moisture tranfer between the capsule shell and its content. J Pharm Sci. 1998;87(5):556–8.
5. Ayenew Z, Paudel A, Rombaut P, Mooter GV. Effect of compression on non-isothermal crystallization behaviour of amorphous indomethacin. Pharm Res. 2012;29(9):2489–98.
6. Ayenew Z, Paudel A, Mooter G. Can compression induce demixing in amorphous solid dispersions? A case study of naproxen–PVP K25. Eur J Pharm Biopharm. 2012;81(1):207–13.
7. Brittain HG. Effects of mechanical processing on phase composition. J Pharm Sci. 2002;91(7):1573–80.
8. Vasconcelos T, Sarmento B, Costa P. Solid dispersions as strategy to improve oral bioavailability of poor water soluble drugs. Drug Discov Today. 2007;12(23–24):1068–75.
9. Patel S, Kaushal AM, Bansal AK. Compression physics in the formulation development of tablets. Crit Rev Ther Drug. 2006;23(1):1–66.
10. Taylor LS, Zografi G. Spectroscopic characterization of interactions between pvp and indomethacin in amorphous molecular dispersions. Pharm Res. 1997;14(12):1691–8.
11. Yoshioka M, Hancock BC, Zografi G. Crystallization of indomethacin from the amorphous state below and above its glass transition temperature. J Pharm Sci. 1994;83(12):1700–5.
12. Forster A, Hempenstall J, Tucker I, Rades T. The potential of small-scale fusion experiments and Gordon–Taylor equation to predict the suitability of drug/polymer blends for melt extrusion. Drug Dev Ind Pharm. 2001;27(6):549–60.
13. Gedde UW. Polymer physics. 1st ed. London: Chapman & Hall; 1995.
14. Qian F, Huang J, Zhu Q, Haddadin R, Gawel J, Garmise R, *et al.* Is a distinctive single Tg a reliable indicator for the homogeneity of amorphous solid dispersion? Int J Pharm. 2010;395(1–2):232–5.
15. Lachman L, Lieberman HA, Kanig JL. Compression and consolidation of powdered solids. In: The theory and practise of Industrial pharmacy. 3 ed. Lachman L, editor: CBS Publisher & Distributors P Ltd; 1987.
16. Kozey VV, Kumar S. Compression behavior of materials: part I. glassy polymers. J Mater Res. 1994;9(10):2717–26.
17. Lee HN, Riggleman RA, Pablo JJD, Ediger MD. Deformation-induced mobility in polymer glasses during multistep creep experiments and simulations. Macromolecules. 2009;42(12):4328–36.
18. Meijer HE, Govaert LE. Mechanical performance of polymer systems: the relation between structure and properties. Prog Polym Sci. 2005;30(8–9):915–38.
19. Lee HN, Paeng K, Swallen SF, Ediger MD. Direct measurement of molecular mobility in actively deformed polymer glasses. Science. 2009;323(5911):231–34.
20. Capaldi FM, Boyce MC, Rutledge GC. Enhanced Mobility Accompanies the Active Deformation of a Glassy Amorphous Polymer. Phys Rev Lett. 2002;89(17):175505-1-4.
21. Marsac PJ, Li T, Taylor LS. Estimation of drug–polymer miscibility and solubility in amorphous solid dispersions using experimentally determined interaction parameters. Pharm Res. 2009;26(1):139–51.
22. Train D. An investigation into the compaction of powders. J Pharm Pharmacol. 1956;8(1):745–61.